# Selection of Suitable Drying Methods and their Characterization for Functional Group Retention and Heavy Metal Uptake in *Sargassum* sp., *Kappaphycus* sp., and *Padina* sp.

**Nazirah Mingu[1], Tengku Ariff Haiekal Tengku Isa[1], Juferi Idris[2], Hasmadi Mamat[3], Sabrina Soloi[1] and Mohd Sani Sarjadi[1]***

[1]Faculty of Science and Technology, Universiti Malaysia Sabah, Jalan UMS, 88400 Kota Kinabalu, Sabah, Malaysia

[2]Faculty of Chemical Engineering, College of Engineering, Universiti Teknologi MARA, Sarawak Branch, Samarahan Campus, Jalan Meranek, 94300 Kota Samarahan, Sarawak, Malaysia

[3]Faculty of Food Science and Nutrition, Universiti Malaysia Sabah, Jalan UMS, 88400 Kota Kinabalu, Sabah, Malaysia

*Corresponding author (e-mail: msani@ums.edu.my)

This study investigated the potential of three seaweed species - *Sargassum* sp., *Kappaphycus* sp., and *Padina* sp. - as biosorbents for removing chromium ($Cr^{6+}$) and cadmium ($Cd^{2+}$) from aqueous solutions. Dried seaweed samples were introduced into metal-containing solutions, and to evaluate their heavy metal adsorption efficacy. Analytical techniques including Fourier Transform Infrared Spectroscopy (FTIR), Inductively Coupled Plasma Optical Emission Spectroscopy (ICP-OES), and Field Emission Scanning Electron Microscopy (FE-SEM) were employed to evaluate the biosorbents. Among the seaweed species studied, *Sargassum* sp. demonstrated the highest efficiency as a heavy metal absorbent. Optimal conditions that enhanced adsorption effectiveness, especially in freeze-dried samples, were identified at pH 6. Freeze-dried samples of *Sargassum* sp. achieved an adsorption efficiency of 75.2 %, highlighting pH 6 as the optimal condition for adsorption across all seaweed species. Functional groups such as -OH, C=C, and S=O were found to play pivotal roles in the biosorption process. Equilibrium uptake studies were conducted using isotherm models, with the Langmuir isotherm demonstrating the best fit, indicating monolayer adsorption. Moreover, adsorption kinetics for *Sargassum* sp. followed a pseudo-second order model, suggesting chemisorption mechanisms involving chemical interactions between sorbates and surface functional groups. Overall, these findings underscore the potential of *Sargassum* sp. as an effective biosorbent for heavy metal removal, and offer insights into optimizing biosorption processes for environmental remediation applications.

**Keywords:** Seaweed*; drying method; Sargassum* sp.*; Kappaphycus* sp.*; and Padina* sp.*;* heavy metals; biosorbents; isotherm; kinetic study

*Received: June 2025; Accepted: October 2025*

In Sabah, heavy metals have contributed to environmental poisoning issues involving rivers, lakes, and the ocean [1-7] due to increasing industrial activity. Given that a substantial proportion of the local population depends on the sea and rivers as their primary sources of sustenance and livelihood, this environmental issue has emerged as an escalating concern within the community. The management and mitigation of heavy metal contamination in wastewater, which poses serious risks to the environment and public health, is a global concern in both urban and rural areas. In urban centres, wastewater often contains effluents from industrial and municipal sources, whereas in rural regions, heavy metals may originate from agricultural practices and small-scale industries [8-11]. Heavy metals accumulate in water bodies, soils, and agricultural areas as a result of wastewater discharged from numerous sources, including houses, businesses and factories, as well as from urban runoff [6-11].

Biosorbents are biological materials that can bind and concentrate heavy metals from aqueous solutions through mechanisms such as ion exchange, complexation, and adsorption onto functional groups present on their cell walls. These are considered a sustainable alternative to conventional treatment methods like chemical precipitation or ion exchange resins as they are inexpensive, environmentally friendly, and can often be regenerated and reused [12-17]. Among various biosorbents, marine algae are particularly attractive due to their high surface area, abundance of polysaccharides, and diverse

functional groups such as hydroxyl, carboxyl, and sulfate that enhance their metal-binding capacity [18-21].

In the present study, marine algae species were selected as biosorbents because they are inexpensive and widely available in Sabah. The coastal regions of Sabah are rich in diverse seaweed resources, including three major groups: rhodophytes (red algae), phaeophytes (brown algae), and chlorophytes (green algae). These species not only provide ecological and economic value but also represent a promising local biomass for the development of low-cost and effective biosorption technologies [2-7].

Seaweed has a lot of potential as a biosorbent for removing heavy metals from contaminated waters due to its wide availability, strong metal-binding capability, and environmentally friendly character [22-24]. Despite this, several challenges and limitations must be addressed before large-scale application can be realised. A critical factor lies in selecting an appropriate seaweed species with a high adsorption efficiency and selectivity for specific heavy metals, as biosorption performance is strongly influenced by functional groups, surface characteristics, and biochemical composition. Environmental parameters such as pH, temperature, and solution chemistry also play a significant role in determining the efficiency of the process [25-27].

Furthermore, optimisation of biosorption requires a deeper understanding of the complex interactions between the physicochemical properties of biosorbents and the target metal ions. Another major limitation is the regeneration and reuse of algae-based biosorbents, as efficient desorption methods are necessary to recover metals without damaging the biosorbent or reducing its functional capacity [28]. Without effective regeneration, secondary waste may be produced, limiting both the economic viability and environmental sustainability of biosorption [29]. Addressing these challenges is therefore essential to advancing the use of seaweed from Sabah as a cost-effective and environmentally friendly material for heavy metal remediation [30-32].

In this study, samples of *Kappaphycus* sp., *Padina* sp., and *Sargassum* sp. were tested to evaluate their ability to adsorb heavy metals, specifically chromium ($Cr^{6+}$) and cadmium ($Cd^{2+}$). A series of systematic experiments were conducted to determine the optimal conditions, including drying methods, initial concentration and pH for adsorption [6, 12]. For the pH experiments, the solutions were adjusted to two levels (pH 4 and 6). Two drying methods, freeze-drying and oven-drying, were employed. The physicochemical properties, surface morphology, and functional groups of the seaweed biosorbents were determined using Fourier Transform Infrared (FTIR) spectroscopy and Field Emission Scanning Electron Microscopy (FE-SEM).

## EXPERIMENTAL

### Chemicals and Materials

The chemicals and materials used in the biosorption process to remove heavy metal chromium ($Cr^{6+}$) and cadmium ($Cd^{2+}$) included ammonium acetate (99 %) (CAS number: 631-61-8) and anhydrous acetic acid (37 %) (CAS number: 64-19-7) from Sigma Aldrich, as well as potassium dichromate and cadmium nitrate from Merck.

**Figure 1** shows the biosorption potential of selected seaweed species, namely *Sargassum* sp., *Kappaphycus* sp., and *Padina* sp. To ensure methodological robustness, the samples underwent controlled preparation and drying processes using both freeze drying and oven drying techniques, enabling a comparison of their effects on structural and functional properties. Subsequent analyses were conducted to evaluate moisture content, loss on drying, and morphological characteristics, complemented by Fourier Transform Infrared (FTIR) spectroscopy for functional group identification. In addition, adsorption experiments were optimised at two acidic conditions (pH 4 and 6) using standard metal solutions of chromium ($Cr^{6+}$) and cadmium ($Cd^{2+}$), thereby providing insight into the influence of environmental parameters on metal uptake efficiency [33].

### Instruments

The instruments used to analyse and characterize samples in this study are listed in **Table 1** below.

### Raw Material Preparation

The samples used in this experiment (**Figure 2**) were *Kappaphycus* sp. and *Padina* sp., which were purchased from Semporna, Sabah, as well as *Sargassum* sp., which was collected at the Outdoor Development Centre (ODEC), Universiti Malaysia Sabah (UMS) **(Figure 3).**

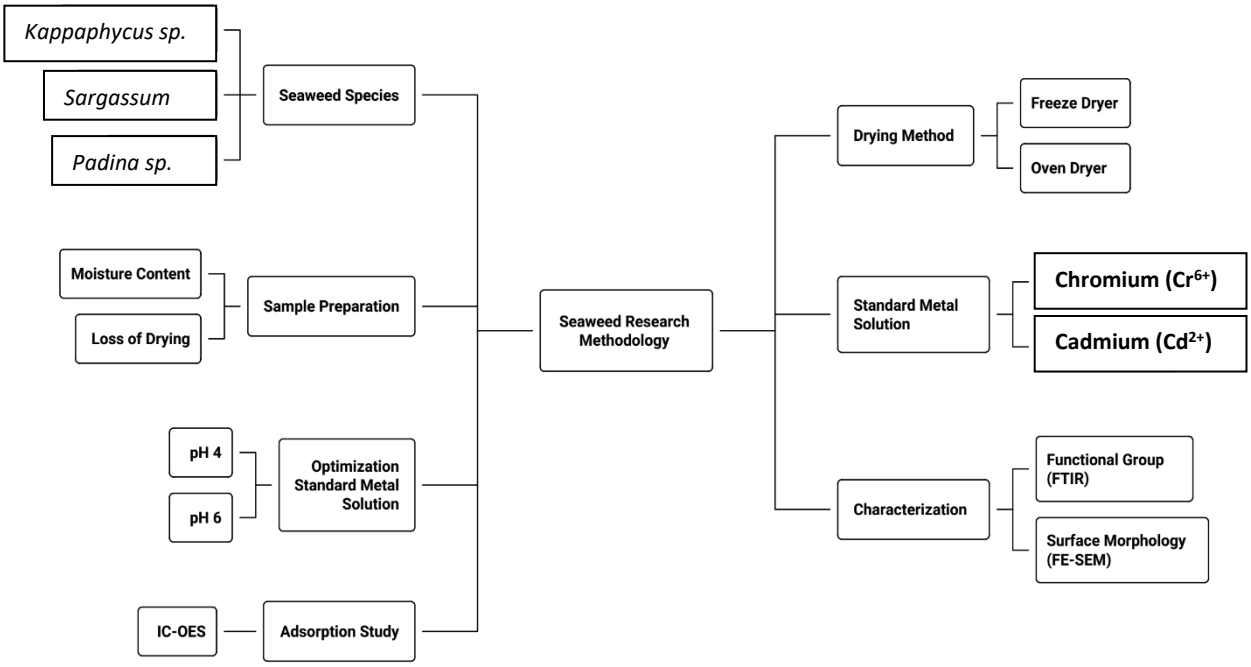


**Figure 1.** Overall experimental design for the evaluation of seaweed species for drying optimisation, characterisation, and adsorption studies.

**Table 1.** List of instruments.

| Instruments | Brand | Purpose |
|---|---|---|
| **Fourier Transmission Infrared Spectroscopy (FTIR)** | BRUKER OPUS | To observe the vibrations of functional groups present in the sample |
| **Inductively Coupled Plasma Optical Emission Spectroscopy (ICP-OES)** | Perkin Elmer | To measure the concentration of heavy metals in the sample before adsorption |
| **Atomic Absorption Spectrometry (AAS)** | Perkin Elmer | To measure the concentrations of heavy metals in the sample after adsorption |
| **Field Emission Scanning Electron Microscope (FESEM)** | JEOL JSM-7900F | To obtain the surface morphology of the sample |


**Figure 2.** Features of three selected seaweed species (a) *Sargassum* sp. (b) *Kappaphycus* sp. (c) *Padina* sp.

**Figure 3.** Collection of *Sargassum* sp. seaweed samples at ODEC, UMS.

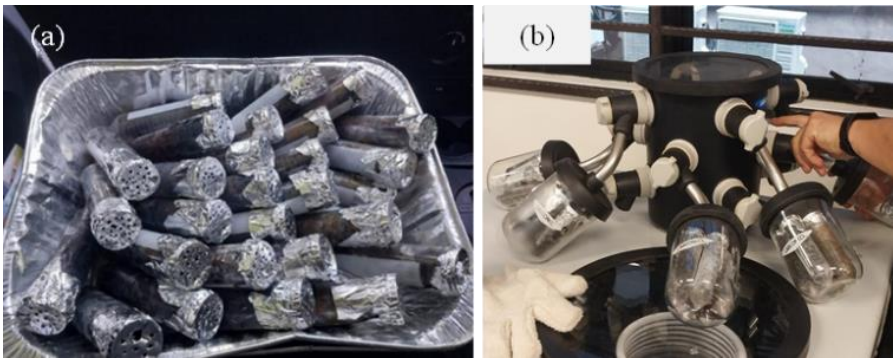


**Figure 4.** (a) Samples were kept in 50 mL centrifuge tubes for preparation before freeze drying (b) Freeze dryer machine.

The collected samples were washed repeatedly with deionized water to remove extraneous material and salts until they reached pH 7. The samples were then dried in an oven at 333 K for 48 h until a constant weight was reached [22-25]. Separate samples were kept in 50 mL centrifuge tubes for preparation before freeze drying (**Figure 4**) [34]. All dried seaweed were powdered using a mixer grinder and sieved through a 1.0 - 1.5 mm pore size sieve and stored in containers for further use [35-37].

**Stock Solutions of Chromium ($Cr^{6+}$) and Cadmium ($Cd^{2+}$)**

Stock solutions of chromium ($Cr^{6+}$) and cadmium ($Cd^{2+}$) were prepared by dissolving cadmium nitrate and potassium dichromate in 100 mL distilled water [38]. The stock solutions (1000 ppm) for both cadmium and chromium were prepared by dissolving 1.3 g of cadmium nitrate in 1000 mL deionized water and 1.0 g of potassium dichromate in 100 mL deionized water.

**The pH Adjustment of Chromium ($Cr^{6+}$) and Cadmium ($Cd^{2+}$) Solutions**

A buffer was used to bring the solution to the desired pH. The buffer solution was prepared by mixing sodium acetate with distilled water. A weak acid, acetic acid was dripped slowly into the aqueous solution of sodium acetate until it reached the desired pH, which was measured using a pH meter. All the solutions were set at two different pH values, 4 and 6. The pH was adjusted periodically to the desired value by adding more buffer or acetic acid solution [39].

The pH values of 4 and 6 were selected to represent mildly acidic environments that are commonly encountered in natural aquatic systems and industrial effluents [22]. Previous studies have demonstrated that pH plays a critical role in modulating the ionisation state of functional groups in seaweed cell walls, such as –OH, –COOH, and –$SO_3H$, which in turn affects their binding affinity towards metal ions [25, 29].

The choice of pH 4 and 6, rather than strongly acidic or alkaline conditions, was made to ensure that the functional groups remained chemically active while still reflecting realistic environmental conditions where biosorption processes typically occur [38]. Furthermore, working within this pH range prevents extensive hydrolysis or degradation of the biomass, which can occur under more extreme pH values, thereby ensuring the structural integrity of the samples during FTIR analysis [38-40].

**Sample Preparation**

A biosorption process was used to carry out the metal ion removal. All three seaweed samples were used in this process. The procedure took 40 min for each replication. The pH and drying method were varied for each sample [25]. The initial concentration of metal solution was set to 1.0 g/1000 mL.

First, 0.2 g of each seaweed was placed in a 50 mL centrifuge tube (**Figure 5**). Then, 15 mL of buffer solution was added into the tube and the mixture was left for 30 min. Then, 15 mL of chromium ($Cr^{6+}$) solution was added. This step was repeated using a cadmium solution instead [39].

**Adsorption Process**

**Table 2** shows the details of the samples used in the batch biosorption study. The study was carried out on a set of centrifuge tubes with 30 mL of various heavy metal ion solutions at various pH levels [26] and drying methods, as shown in **Figure 6**. In order to conduct all sorption tests (Table 1), each centrifuge tube was immersed in an ultrasonic bath at ambient temperature for 30 min at 40 kHz [27]. The tube was then centrifuged at 3500 rpm for 10 min at ambient temperature to complete phase separation.

Using a syringe, the solution at the top of the centrifuge tube was removed and collected in a test tube. This solution was diluted to 1.0 ppm before evaluation [27].

In addressing the optimisation of the drying methods (freeze drying versus oven drying), several controlled variables were carefully standardised to ensure that the differences observed could be attributed solely to the drying techniques employed. The same seaweed species (*Kappaphycus* sp*., Padina* sp*., and Sargassum* sp.) were utilised, and each sample was prepared with identical initial fresh weights, comparable moisture content, and uniform pre-treatment procedures (washing, cutting, and handling). Furthermore, all experiments were performed under consistent laboratory conditions, using the same equipment settings and maintaining uniform post-drying storage conditions prior to FTIR analysis [38].

This methodological control is essential because the reliability of drying optimisation strongly depends on minimising external variability, as highlighted in previous studies [40-42, 47]. By ensuring that these parameters are standardised, the influence of confounding factors is reduced, thereby allowing the observed differences in spectral and compositional outcomes to be attributed primarily to the drying method applied.


**Figure 5.** (a) The adsorbent was placed in a standard metal solution in a 50 mL centrifuge tube with a concentration of 1000 ppm; (b) The sample was immersed in an ultrasonic bath for 30 min at 40 kHz; (c) Sample ready for centrifuge.

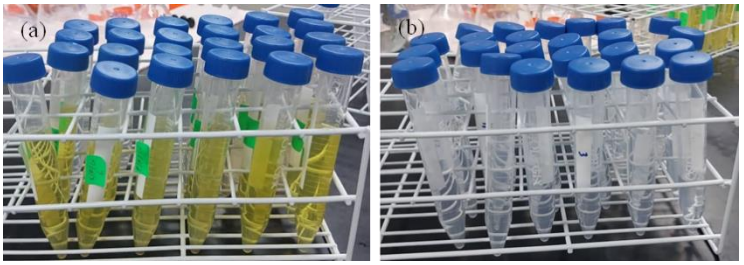


**Figure 6.** Batch biosorption tests in centrifuge tubes with 30 mL of a heavy metal ion solution at different pH levels: (a) before dilution; (b) after dilution.

**Table 2.** Sample data based on seaweed species, drying method, heavy metal, and pH.

| Bil. | Sample code | Sample detail | | | |
|---|---|---|---|---|---|
| | | Seaweed species | Drying method | Heavy metal | pH |
| 1 | S1 | *Kappaphycus* sp. | Freeze dryer | Chromium ($Cr^{6+}$) | 6 |
| 2 | S2 | *Kappaphycus* sp. | Oven dryer | Chromium ($Cr^{6+}$) | 6 |
| 3 | S3 | *Padina* sp. | Oven dryer | Chromium ($Cr^{6+}$) | 6 |
| 4 | S4 | *Padina* sp. | Freeze dryer | Chromium ($Cr^{6+}$) | 6 |
| 5 | S5 | *Sargassum* sp. | Freeze dryer | Chromium ($Cr^{6+}$) | 6 |
| 6 | S6 | *Sargassum* sp. | Oven dryer | Chromium ($Cr^{6+}$) | 6 |
| 7 | S7 | *Padina* sp. | Freeze dryer | Chromium ($Cr^{6+}$) | 4 |
| 8 | S8 | *Padina* sp. | Oven dryer | Chromium ($Cr^{6+}$) | 4 |
| 9 | S9 | *Sargassum* sp. | Oven dryer | Chromium ($Cr^{6+}$) | 4 |
| 10 | S10 | *Sargassum* sp. | Freeze dryer | Chromium ($Cr^{6+}$) | 4 |
| 11 | S11 | *Kappaphycus* sp. | Oven dryer | Chromium ($Cr^{6+}$) | 4 |
| 12 | S12 | *Kappaphycus* sp. | Freeze dryer | Chromium ($Cr^{6+}$) | 4 |
| 13 | S13 | *Padina* sp. | Freeze dryer | Cadmium ($Cd^{2+}$) | 4 |
| 14 | S14 | *Padina* sp. | Oven dryer | Cadmium ($Cd^{2+}$) | 4 |
| 15 | S15 | *Sargassum* sp. | Freeze dryer | Cadmium ($Cd^{2+}$) | 4 |
| 16 | S16 | *Sargassum* sp. | Oven dryer | Cadmium ($Cd^{2+}$) | 4 |
| 17 | S17 | *Kappaphycus* sp. | Oven dryer | Cadmium ($Cd^{2+}$) | 4 |
| 18 | S18 | *Kappaphycus* sp. | Freeze dryer | Cadmium ($Cd^{2+}$) | 4 |
| 19 | S19 | *Padina* sp. | Freeze dryer | Cadmium ($Cd^{2+}$) | 6 |
| 20 | S20 | *Padina* sp. | Oven dryer | Cadmium ($Cd^{2+}$) | 6 |
| 21 | S21 | *Kappaphycus* sp. | Oven dryer | Cadmium ($Cd^{2+}$) | 6 |
| 22 | S22 | *Kappaphycus* sp. | Freeze dryer | Cadmium ($Cd^{2+}$) | 6 |
| 23 | S23 | *Sargassum* sp. | Freeze dryer | Cadmium ($Cd^{2+}$) | 6 |
| 24 | S24 | *Sargassum* sp. | Oven dryer | Cadmium ($Cd^{2+}$) | 6 |

**Analysis Techniques**

In this study, a series of equipment was used to analyse the sample before and after the biosorption process. The sample was centrifuged to remove the biosorbent, and analyzed by ICP-OES to determine the concentration of chromium ($Cr^{6+}$) and cadmium ($Cd^{2+}$) ions present. FE-SEM was used to analyze the change in morphology of the sample before and after the biosorption process [20, 44,47]. FTIR was used to determine the functional groups in the loaded and unloaded samples [19-22, 47-49].

*Fourier Infrared Transform Spectroscopy (FTIR)*

FTIR was used to analyse the functional groups present in *Kappaphycus* sp., *Padina* sp., and *Sargassum* sp. before and after the biosorption process. The changes in vibration wavelengths of the functional groups in the samples were also measured. The samples were analysed at 650 to 4000 $cm^{-1}$. Each dry sample was ground to a fine powder before FTIR analysis. The background from the pure KBr scan was automatically removed from the sample spectra [50-52]. The peaks for each functional group were smoothed using automatic smooth correct, and peaks of interest were labelled [53].

*Field Emission Scanning Electron Microscopy (FE-SEM)*

FE-SEM was used to analyze the surface morphology of the samples [54]. The texture and morphology of *Kappaphycus* sp., *Padina* sp., and *Sargassum* sp. were scanned before and after treatment. This technique allowed direct observation of the sample microstructure that changed due to the biosorption process [55].The 100x - 500x magnification power of the FE-SEM allows observation of texture and morphology characteristics which are not visible to the human eye [39].

*Inductively Coupled Plasma Optical Emission Spectroscopy (ICP-OES)*

ICP-OES is an analytical method that determines the concentration of certain elements that exist in a sample. Centrifugation was used to separate the metal solution from the biosorbent for 15 min at a speed of 4000 rpm. Before analysis, the solution was put through an acid digestion process to dissolve the analytes and decompose any solids present in the solution [54]. The aim of this process was to avoid contamination of the samples. In this study, ICP-OES was used to determine the concentrations of chromium

($Cr^{6+}$) and cadmium ($Cd^{2+}$) in *Kappaphycus* sp., *Padina* sp., and *Sargassum* sp. [26, 55]

**Adsorption Study of Selected Samples**

One sample from the best parameter was tested again to study the adsorption rate of the seaweed. 0.2 g of the selected sample was added to an Erlenmeyer flask. 15 mL of a buffer solution was poured into the flask which was then left for 30 min. 15 mL of a 100 ppm metal solution was then added to the mixture. The flask was agitated using a rotary shaker for 3 h. Every 30 min, 5 mL of the solution was transferred into a test tube using a syringe. The solution in the test tube was diluted with distilled water and sent for ICP-OES analysis to determine the heavy metal content in the solution [52-53, 56].

## RESULTS AND DISCUSSION

**Comparison of Drying Methods**

Two drying methods were used to prepare the seaweed samples, namely freeze drying and oven drying. The results indicated notable differences in drying loss and moisture retention depending on the method used. Freeze drying is generally recognised as a more effective technique for preserving the structural and biochemical integrity of biological materials, as the removal of water occurs at low temperatures under vacuum, thereby minimising thermal damage [50, 52-54]. By contrast, oven drying exposes samples to elevated temperatures, which accelerate moisture removal but may also induce surface shrinkage, structural collapse, and partial degradation of heat-sensitive compounds [50, 52]. These differences explain the variations observed in the dried seaweed samples.

**Moisture Content**

Moisture content is a critical factor influencing the quality, stability, and shelf life of biosorbents (**Table 3**). A lower moisture content is generally associated with extended shelf life, as microbial growth and enzymatic activity are reduced under drier conditions [46-48]. In this study, Padina sp. exhibited the highest moisture content (91.64 %), followed by *Sargassum* sp. (90.35 %) and *Kappaphycus* sp. (86.29 %). These values are relatively high compared to the typical moisture content reported for fresh seaweeds, which often ranges between 70 % and 90 % depending on species, environment, and harvesting conditions [22].

The slightly lower value for *Kappaphycus* sp. may be attributed to its high carrageenan content, which influences water binding and facilitates more efficient water removal during drying [37-39]. In contrast, *Padina* sp. retained more moisture, consistent with previous observations that it possesses denser cell walls with calcium carbonate deposits, which affect drying behaviour [39]. Additionally, the drying method contributes to variations in moisture removal, e.g., oven drying at elevated temperatures enhances evaporation but may alter the chemical groups involved in water binding through processes such as chemisorption [44].

**Loss on Drying**

Loss on drying is the reduction in sample weight in w/w percentage due to water and volatiles. The sample may break down during drying and emit decomposition products. Therefore, the water content may be determined by a gravimetric technique assuming no breakdown happens and volatiles are absent. **Figure 7** shows the drying rates for the different seaweed species [44-46]. The drying rate for *Sargassum* sp. became constant at 240 min, indicating that all water and volatile compounds in the sample had been completely removed. The removal rate rose sharply from 0 % to 91.46 %, with the most substantial increase occurring between 0 and 120 min. The rate then plateaued, showing only a slight increase between 180 minutes (91.46 %) and 300 minutes (92.10 %), suggesting that most of the moisture was removed early.

**Table 3.** Moisture content of the biosorbent.

| Sample | Moisture (% Weight) |
|---|---|
| *Sargassum* sp. | 90.35 |
| *Kappaphycus* sp. | 86.29 |
| *Padina* sp. | 91.64 |

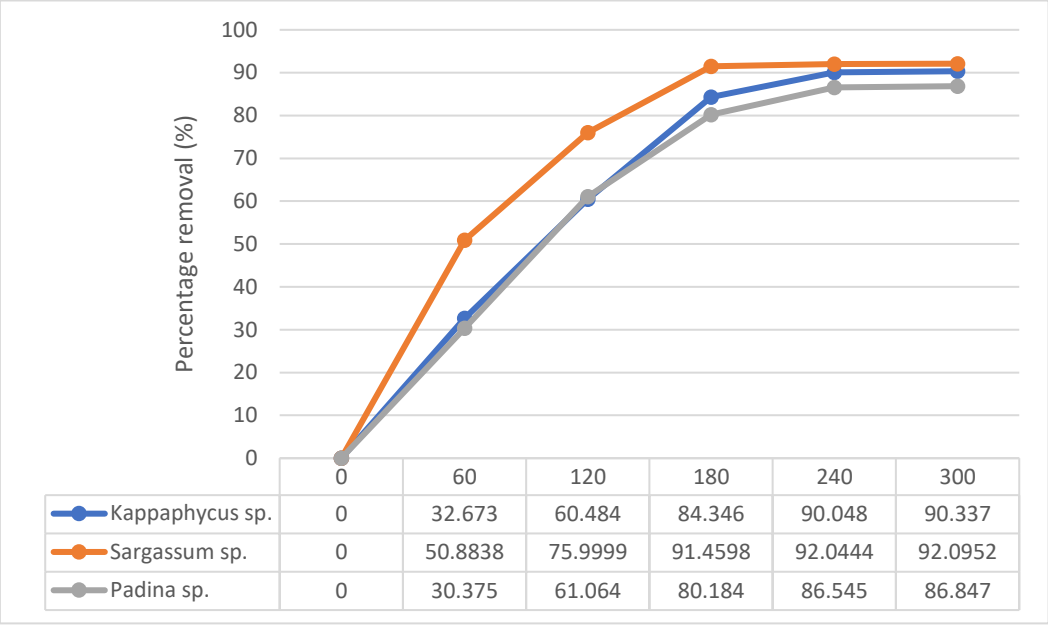


**Figure 7.** Drying rates of the seaweed species.

*Kappaphycus* sp. followed a similar trend, with removal increasing from 0 % to 84.35 % in 180 minutes [16, 26, 42]. After that, the rate slowed considerably, reaching 90.05 % at 240 minutes and only increasing marginally to 90.34 % at 300 minutes. For *Padina* sp., the drying rate was also steep between 0 and 180 min, rising from 0 % to 80.18 %. The increase slowed after that, with a final percentage removal of 86.85 % in 300 minutes. *Padina* sp. showed a significantly lower moisture content compared to *Kappaphycus* sp. and *Sargassum* sp., and this might be due to differences in their cell wall composition.

A comparative nutritional study reported that *Sargassum* sp. contained 8.5 % moisture and 73.5 % carbohydrates, while *Padina* sp. had slightly higher moisture (9.7%) with 66.8% carbohydrates [24, 35]. Furthermore, a comprehensive review on seaweed cell-wall polysaccharides noted that algal cell walls can consist of up to 50–76 % polysaccharides (e.g., alginate, fucoidan), which are critical to structural integrity and water retention [36]. Together, these observations suggest that species-specific differences in polysaccharide composition underpin variability in moisture retention among brown seaweeds [9, 24, 31, 33].

The drying behaviour of seaweed samples exhibited a characteristic trend of an initial rapid moisture loss followed by a gradual reduction in drying rate. During the first 180 min, the moisture removal rate was highest as the majority of free water located on the surface and within intercellular spaces evaporated. This stage corresponds to the constant rate period, where drying is largely governed by external conditions such as temperature and airflow [49]. The subsequent decline in drying rate after 180 min indicates the transition into the falling rate period. In this stage, the remaining moisture is more tightly bound within the seaweed matrix, and its removal becomes diffusion-limited [46].

The slow drying phase is strongly influenced by the structural and biochemical properties of seaweed. Seaweed contains high amounts of hydrocolloids (alginate in *Sargassum*, carrageenan in *Kappaphycus*, and fucoidan in *Padina*) which have strong water-binding capacities [51]. These polysaccharides retain water through hydrogen bonding and matrix entrapment, thereby slowing down the drying process as evaporation progresses. Similar findings have been reported for other hydrocolloid-rich biomasses, where bound water requires significantly higher energy for desorption compared to free water [6-7]. This explains the plateau observed at the later stages of drying, when moisture diffusion through the dense polysaccharide network becomes the rate-limiting step.

A comparison between oven drying and freeze drying further highlights the importance of the drying method on moisture removal. Oven drying relies on convective heat transfer, which accelerates the removal of free water, but can cause structural collapse and reduced diffusion pathways during the bound water

stage [48]. In contrast, freeze drying preserves cellular integrity by sublimating ice directly, leading to higher porosity and improved water removal efficiency in later stages [50]. Consequently, while both methods show a rapid initial drying phase followed by a plateau, freeze-dried samples generally achieve lower residual moisture content and better retention of bioactive compounds, making the method preferable for high-value seaweed applications.

**Sample Preparation**

Understanding the properties of the biosorbent is crucial in determining whether it needs pre-treatment to enhance its ability to associate with heavy metals. The dried samples were ground using a mechanical blender to pulverize the leaves, stems, and roots into smaller units ranging from fragments to a fine powder (**Figure 8**).

Active sites for adsorption in the sample may exist either on the surface of the biosorbent or inside the cell. Grinding the sample allows the heavy metal ions to adsorb onto the interior of the biosorbent [17].

**FTIR Analysis**

Twelve samples of seaweed were analyzed using FTIR. The sample was divided into two groups, in which the functional groups were present in the biosorbent after drying and after adsorption. **Figure 9** shows the FTIR spectra of the *Sargassum* sp. samples obtained by two different drying methods: freeze drying and oven drying [39]. Based on these spectra, both drying methods still preserved the OH, C=O and C-O functional groups (Table 4).

Notably, the oven-dried sample displayed a more prominent band at 1123 $cm^{-1}$, which can be attributed to S=O stretching of sulphate esters, a common feature of fucoidan in brown seaweeds. The band at 1022 $cm^{-1}$ indicated the presence of C–O and C–O–C vibrations from polysaccharides. Overall, both spectra confirmed the typical fingerprints of brown seaweed polysaccharides, particularly hydroxyl, carboxylate, and glycosidic groups, with the oven-dried sample showing a stronger sulphate ester signal and a slight shift in the hydroxyl band, reflecting the influence of drying conditions on the molecular structure [36, 39-40].

This preservation can be theoretically explained by the relatively mild conditions involved in freeze drying and controlled-temperature oven drying. Freeze drying removes water via sublimation at low temperatures, minimizing thermal degradation and maintaining molecular integrity [18]. Similarly, oven drying at moderate temperatures may not reach the activation energy required to break down these functional groups, especially when exposure time is limited [19]. The preservation of functional groups such as –OH and C=O is critical, as they are often associated with the biological activity and adsorption capacity of seaweed-derived materials. Therefore, the consistent spectral patterns in both drying methods suggest that the structural and functional integrity of *Sargassum* sp. was retained, aligning with previous findings that reported minimal chemical changes in the polysaccharides and phenolic compounds under controlled drying processes [20].

Table 3 presents the FTIR peak data, and the corresponding functional groups identified in samples of *Kappaphycus* sp., *Sargassum* sp., and *Padina* sp. under different treatment conditions, including drying methods (freeze drying and oven drying) and pH conditions (pH 4 and pH 6). The spectra showed consistent functional groups across treatments, notably –OH stretching, C=O and C–O stretches, C=C (benzene ring), and minor peaks related to S=O and N–H bending. Based on Table 3, the freeze drying method preserved more functional groups. With oven drying, many functional groups disappeared, especially the OH group. Thus, freeze drying is better at preserving nutritional content and functional groups [50]. The intensity of the OH peak after oven drying was lower than after freeze drying. There was no disappearance of functional group peaks, only the peak intensities were different [32].

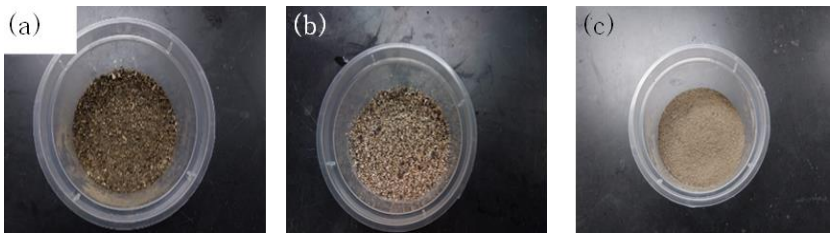


**Figure 8.** Preparation of dried adsorbent samples of (a) *Sargassum* sp.; (b) *Kappaphycus* sp. and (c) *Padina* sp.

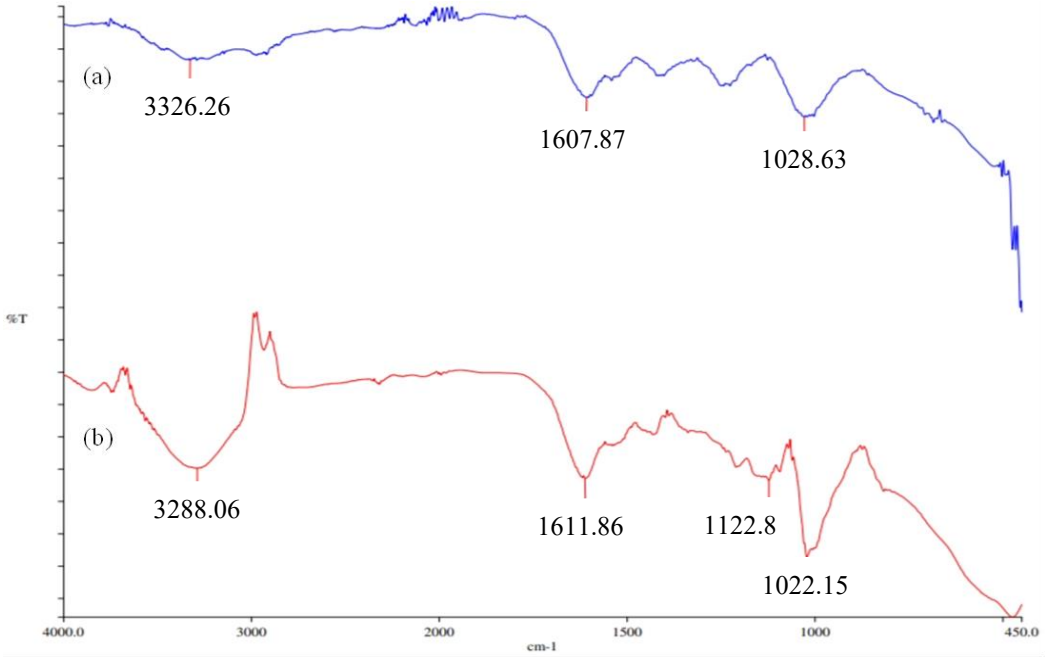


**Figure 9.** FTIR spectra of *Sargassum* sp. samples obtained by different drying techniques: (a) freeze drying; (b) oven drying.

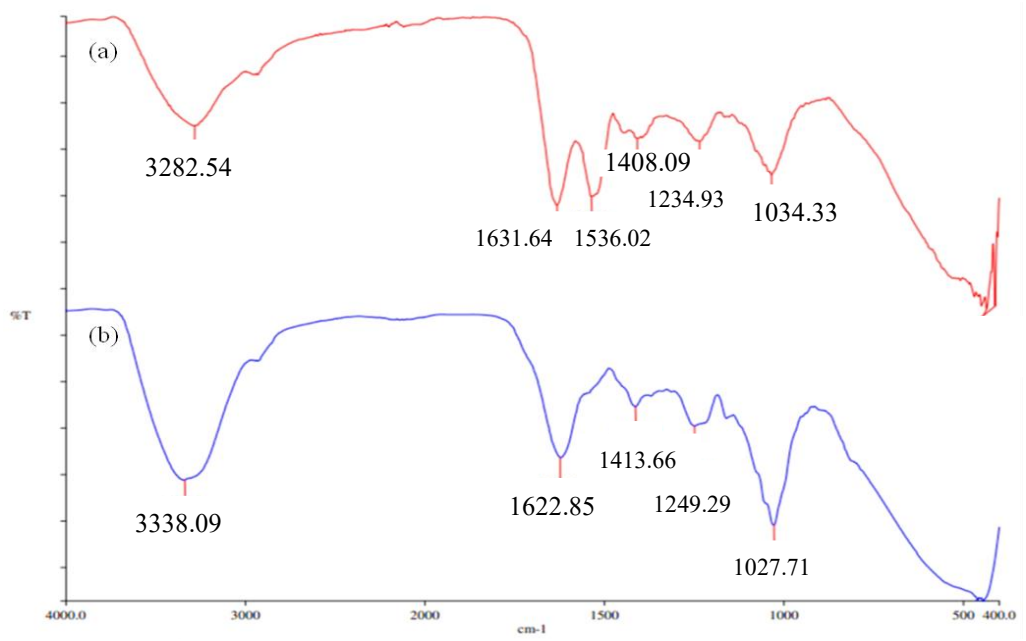


**Figure 10.** FTIR spectra of *Sargassum* sp. samples after adsorption at different pH (a) pH 4; (b) pH 6.

**Figure 10** shows the FTIR spectra of *Sargassum* sp. after adsorption at pH 4 and 6. The functional groups present in the spectra were OH, NH, $-SO_3$ and -CO. **Table 4** contains the FTIR spectroscopic data for *Sargassum* sp., *Kappaphycus* sp. *and Padina* sp. after adsorption in different pH solutions [32, 50]. After adsorption, the spectra showed broad bands at 3200 - 3400 $cm^{-1}$ which indicated the bonded OH and NH groups present in the biosorbent. The peak at 1600 - 1650 $cm^{-1}$ indicates C-O asymmetrical stretching after adsorption. The band at 1200 - 1300 $cm^{-1}$ was related to $-SO_3$ stretching. Peaks at 1050 - 1300 $cm^{-1}$ indicated the C-O stretching of ether groups.

In comparison, the spectrum at pH 6 retained the characteristic O–H stretching band in the region of 3320 - 3330 $cm^{-1}$ and the carboxylate-associated band around 1630 $cm^{-1}$. However, the distinct peak at 1536 $cm^{-1}$ which was observed at pH 4, was absent here.

The disappearance of this peak may be explained by changes in the ionisation state of amino and amide groups at higher pH, where deprotonation reduces their infrared absorption intensity, thereby diminishing their spectral visibility [50].

The differences observed in these spectra are due to heavy metals binding to the functional groups. The interaction of a heavy metal ion with the active site of an adsorbent may be the source of new adsorption bands, changes in adsorption strength and wavenumber shifts [13].This phenomenon may also occur due to the solvents present, such as the buffer solution.

Overall, FTIR analysis indicated that the main functional groups were well preserved in all three seaweed species across drying methods and pH conditions. This suggests that the structural composition of bioactive compounds, especially those responsible for adsorption activity such as polysaccharides and phenolics, remained largely unaffected. These findings are consistent with previous literature which reported that moderate oven temperatures and freeze drying were effective at maintaining the molecular stability of seaweed-derived materials [19][32].

Based on Table 4 and Figure 11 (FTIR spectra), the comparison between samples of *Sargassum* sp. showed similar functional groups in both the freeze-dried and oven-dried samples, with slight differences in wavenumber. The O–H stretching band appeared at 3326 $cm^{-1}$ in the freeze-dried sample and at 3288 $cm^{-1}$ in the oven-dried sample, indicating that hydrogen bonding was better preserved during freeze drying [25-26, 36]. The C=O stretching peak was observed at 1607 $cm^{-1}$ (freeze-dried) and 1611 $cm^{-1}$ (oven-dried), representing carbonyl or amide I groups, with only minor shifts between the methods. The C–O stretching, related to polysaccharides such as alginate and fucoidan, was detected at 1029 $cm^{-1}$ in the freeze-dried sample and at 1022 $cm^{-1}$ in the oven-dried sample. These small shifts suggest that freeze drying maintains the structural integrity of hydroxyl, carbonyl, and polysaccharide groups more effectively, whereas oven drying may cause some degradation due to heat exposure [44].

In this study, FTIR analysis was conducted to identify the major functional groups present in the investigated seaweed species. As summarised in **Table 4**, the spectra of *Sargassum* sp., *Kappaphycus* sp., and *Padina* sp. consistently revealed the presence of characteristic peaks corresponding to -OH stretching, C=O stretching, C–O stretching, and S=O stretching, among others. These peaks indicate a high degree of similarity in the chemical composition across the species analysed [16, 24, 26].

**Table 4.** FTIR data and corresponding functional groups observed in samples of *Sargassum* sp., *Kappaphycus* sp. *and Padina* sp.

| Seaweed | Wavenumber ($cm^{-1}$) | | | | Functional group |
|---|---|---|---|---|---|
| | Freeze dry | Oven dry | pH 4 | pH6 | |
| ***Kappaphycus* sp.** | 3388.89 | - | 3336.05 | 3274.20 | -OH stretching |
| | - | - | 1059.54 | 1032.13 | C=C (benzene) |
| | - | - | - | - | C=O stretch |
| | 1028.21 | 921.20 | 1610.97 | 1634.37 | C-O stretch |
| | - | - | - | - | -NH bending |
| | 846.91 | - | | 845.01 | S=O stretch |
| ***Sargassum* sp.** | 3326.26 | 3288.06 | 3282.54 | 3338.09 | -OH stretching |
| | - | - | | | C=C (benzene) |
| | 1607.87 | 1611.86 | 1631.64 | 1622.85 | C=O stretch |
| | 1028.63 | 1022.15 | 1029.93 | 1027.75 | C-O stretch |
| | - | - | - | - | -NH bending |
| | - | - | - | - | S=O stretch |
| ***Padina* sp.** | 3274.30 | 3288.47 | 3388.47 | 3337.43 | -OH stretching |
| | - | - | - | - | C=C (benzene) |
| | - | - | 1600.87 | 1615.67 | C=O stretch |
| | - | - | 1027.75 | 1027.78 | C-O stretch |
| | - | - | - | - | -NH bending |
| | 854.13 | 854.42 | - | 853.65 | S=O stretch |

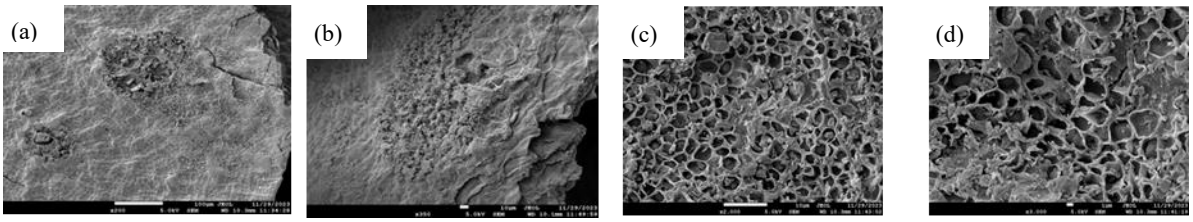


**Figure 11**. FE-SEM images of the surface morphology of freeze-dried *Sargassum* sp. at different magnifications: (a)100x (b) 500x (c) 1000x (d) 5000x.

Due to these spectral similarities, it was deemed unnecessary to present all the spectra in the report, as such repetition would not contribute additional scientific value. Previous studies have also emphasised that when multiple samples exhibit comparable spectral patterns, representative spectra are sufficient to illustrate the chemical functionalities present [27]. Instead, only spectra with significant distinctions are presented, thereby ensuring clarity while avoiding redundancy. This approach not only improves the readability of the results but also directs attention to the spectral features most relevant to the study objectives [6-7, 45].

**Surface Morphology Studies**

Twelve samples of seaweed were analyzed using Field Emission Scanning Electron Microscopy (FE-SEM). The samples were divided into two main groups, to determine the surface morphology of the seaweed after drying and adsorption. There were significant findings based on particle size, surface, shape, and pore distribution.

*Surface Morphology of Seaweed After Drying*

FE-SEM images of the surface morphology of freeze-dried *Sargassum* sp. samples are shown in **Figure 11.** Based on the FE-SEM micrographs, the average particle size of the adsorbent was 10 µm. The surface of the adsorbent appeared rough but the cell walls were still maintained. This was due to the freeze drying method that preserved the cell structure while eliminating water. The pores were visibly large and abundant.

The difference in moisture content among the seaweed samples can be explained by their cell wall composition, as reported in the literature. *Kappaphycus* sp. is rich in carrageenan, a hydrophilic sulphated galactan that efficiently binds water [37]. *Sargassum* sp. contains alginates and fucoidans, which are also highly hydrophilic [36, 43]. In contrast, *Padina* sp. generally has a lower proportion of these polysaccharides and a more rigid wall structure, often with calcium carbonate deposits and phenolic compounds, thereby reducing its capacity to retain water [39, 42].

FE-SEM images of the surface morphology of oven dried *Sargassum* sp. samples are shown in **Figure 12.** Based on these micrographs, the average particle size of the adsorbent was 10 µm. The surface of the adsorbent appeared rough and wrinkled. The cell wall of the adsorbent looked wrinkled due to the uneven high temperatures of the oven drying method [44-47]. The abundant pores appeared flaccid.

Based on these observations, the adsorbent particles were approximately 10 µm in diameter. The surface of the oven-dried *Sargassum* sp. appeared notably rough and wrinkled. This morphological distortion likely results from the uneven application of high temperatures during oven drying, which can deform the cell wall matrix by causing moisture evaporation and structural collapse [44]. Similar heat-induced surface damage has been documented in other biological samples, where excessive thermal treatment leads to surface deformation and fibrous collapse [35-37].

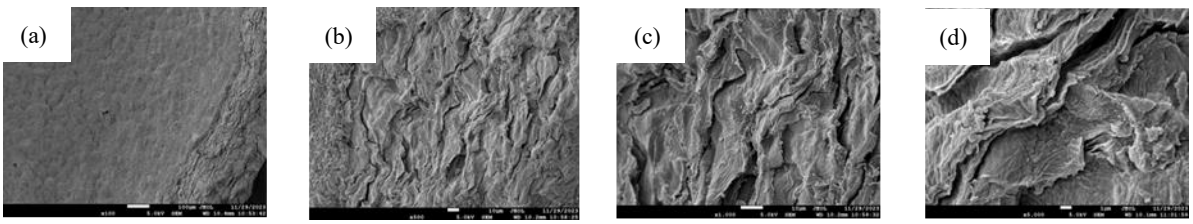


**Figure 12.** FE-SEM images of the surface morphology of oven-dried *Sargassum* sp. at different magnifications: (a)100x (b) 500x (c) 1000x (d) 5000x.

FE-SEM images of the surface morphology of freeze-dried *Kappaphycus* sp. samples are shown in **Figure 13.** Based on the FE-SEM micrographs, the particle size of the adsorbent was 10 µm. The surface of the adsorbent appeared smooth, while the cell walls were still maintained. The vein of the biosorbent can be seen in the micrograph. This is due to the freeze drying method that preserved the cell structure by just eliminating water. The pores were large and abundant. The small particles were the salt residue from evaporated seawater [40].

The attribution to cell wall composition is supported by our FESEM observations. The freeze-dried samples retained more porous and intact structures, whereas oven-dried Sargassum sp. displayed wrinkled and roughened surfaces, suggesting thermal damage to the cell walls. Although we did not chemically quantify polysaccharides, these morphological findings are consistent with the literature that links carrageenan in *Kappaphycus* sp. to higher water retention [37, 42] and alginate/fucoidan in *Sargassum* to similar hydrophilic behaviour [43]. In contrast, *Padina* sp. has been reported to exhibit denser walls and calcium carbonate deposits, which reduce water binding [39].

FE-SEM images of the surface morphology of oven dried *Kappaphycus* sp. are shown in **Figure 14.** Based on the FE-SEM micrographs, the average particle size of the adsorbent was 10 µm. The surface of the adsorbent appeared rough, wrinkled and rigid. Uneven heat distribution during oven drying can cause the outer layer of the adsorbent to become fragile, hard, and wrinkled [28]. There were no pores visible at the surface of the biosorbent due to the mild shrinkage.

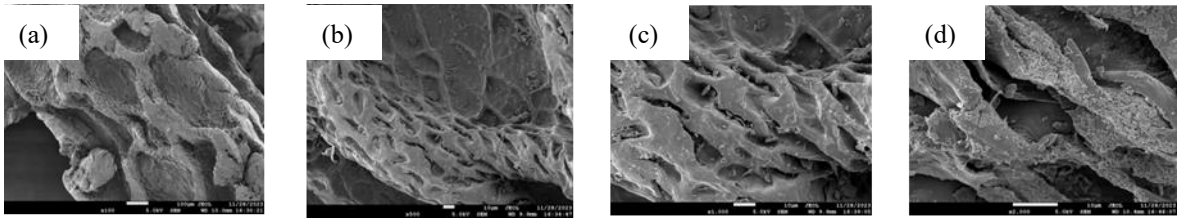


**Figure 13.** FE-SEM images of the surface morphology of freeze-dried *Kappaphycus* sp. at different magnifications: (a)100x (b) 500x (c) 1000x (d) 5000x.

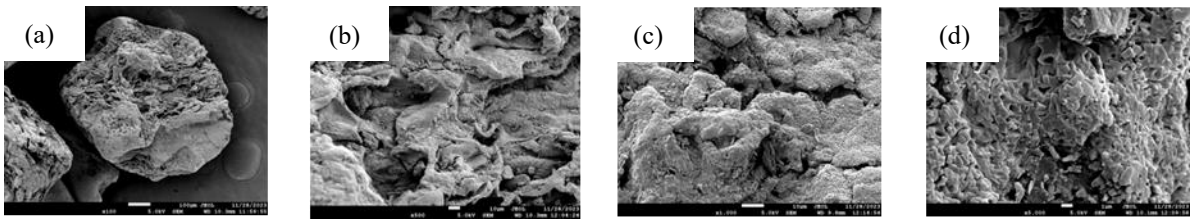


**Figure 14.** FE-SEM images of the surface morphology of oven dried *Kappaphycus* sp. at different magnifications: (a)100x (b) 500x (c) 1000x (d) 5000x.

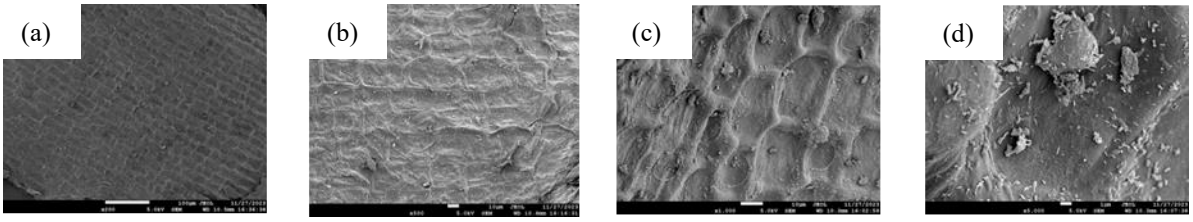


**Figure 15.** FE-SEM images of the surface morphology of freeze-dried *Padina* sp. at different magnifications: (a)100x (b) 500x (c) 1000x (d) 5000x.

FE-SEM images of the surface morphology of freeze-dried *Padina* sp. samples are shown in **Figure 15.** Based on the FE-SEM micrographs, the average particle size of the adsorbent was 10 µm. The surface of the adsorbent appeared smooth and the cellular structure of the biosorbent was still well preserved. Freeze drying makes it possible to dispose of moisture in an effective manner without generating any substantial structural changes or inflicting any damage to the cellular structure of the food [28]. There were no visible pores at the surface of the biosorbent.

FE-SEM images of the surface morphology of oven dried *Padina* sp. samples are shown in **Figure 16.** Based on the FE-SEM micrographs, the average particle size of the adsorbent was 10 µm. The surface of the adsorbent appeared rough and wrinkled. The surface had shrunk due to high temperature drying. This process damages the cellular structure of the biosorbent. There were no pores visible at the surface of the biosorbent, while the crystal-like residue on the surface of the biosorbent was salt from seawater due to insufficient washing.

The conclusion that can be made from the FE-SEM images is that the drying method affects the surface morphology of the biosorbent in terms of particle size, surface, and pore distribution after adsorption.

*Surface Morphology of Seaweed After Adsorption at Different pH*

**Figures 17** to **22** display the surface morphology images of the biosorbent after adsorption at pH 4 and 6. The images show the transformation that occured at the biosorbent's surface, shifting from a wrinkled and rough texture to a smooth and turgid one. This shows that the heavy metals in the metal solution were adsorbed into the biosorbent. This process allowed functional groups present on the biosorbent's surface to bind to heavy metal ions. The particle size of the biosorbent increased due to the adsorption process. The pore distribution at the biosorbent surface was less after adsorption because of pore filling.

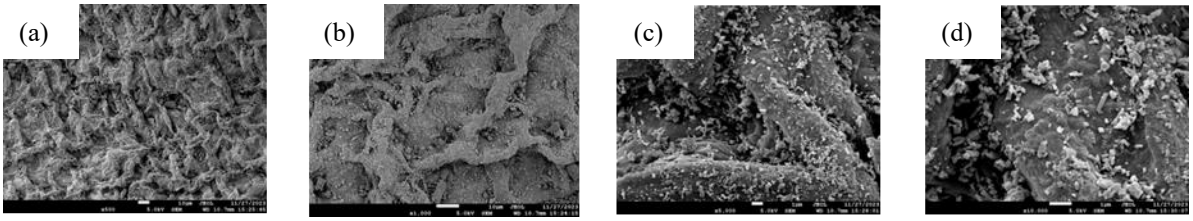


**Figure 16.** FE-SEM images of the surface morphology of freeze-dried *Padina* sp. at different magnifications: (a)100x (b) 500x (c) 1000x (d) 5000x.

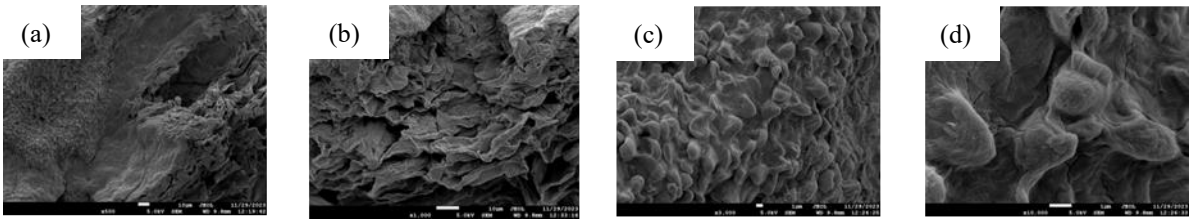


**Figure 17.** FE-SEM images of the surface morphology of *Sargassum* sp. after adsorption at pH 4, at different magnifications: (a) 500x (b) 1000x (c) 3000x (d) 5000x.

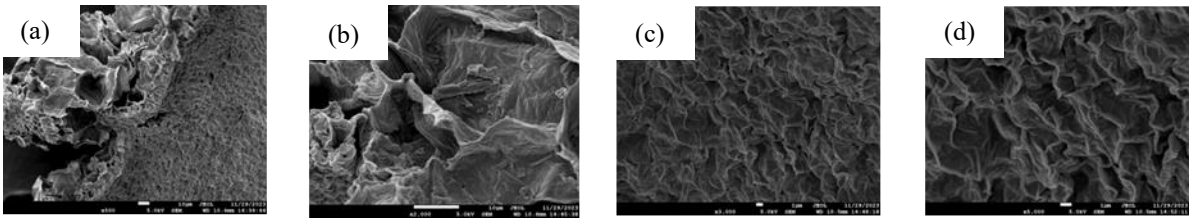


**Figure 18.** FE-SEM images of the surface morphology of *Sargassum* sp. after adsorption at pH 6, at different magnifications: (a) 500x (b) 2000x (c) 3000x (d) 5000x.

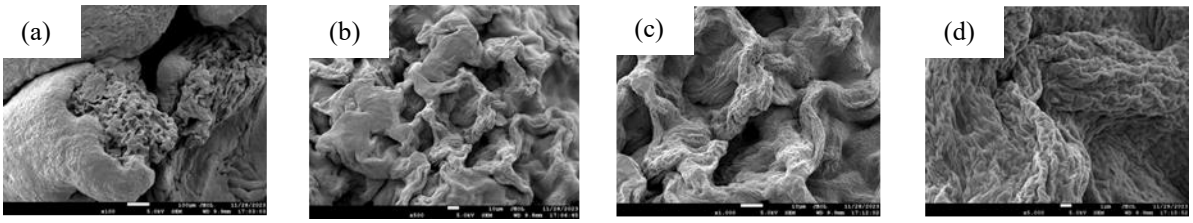


**Figure 19.** FE-SEM images of the surface morphology of *Kappaphycus* sp. after adsorption at pH 4, at different magnifications: (a)100x (b) 500x (c) 1000x (d) 5000x.

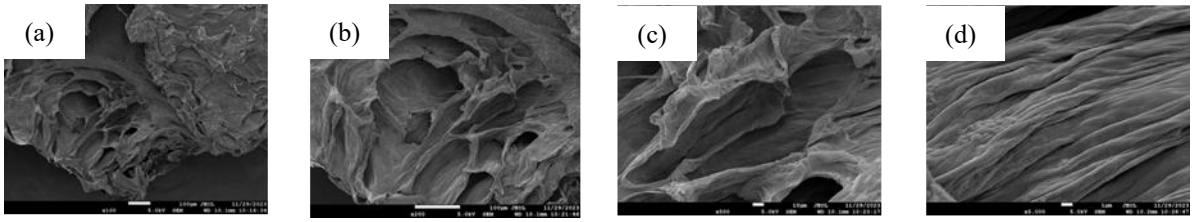


**Figure 20.** FE-SEM images of the surface morphology of *Kappaphycus* sp. after adsorption at pH 6, at different magnifications: (a)100x (b) 200x (c) 500x (d) 5000x.

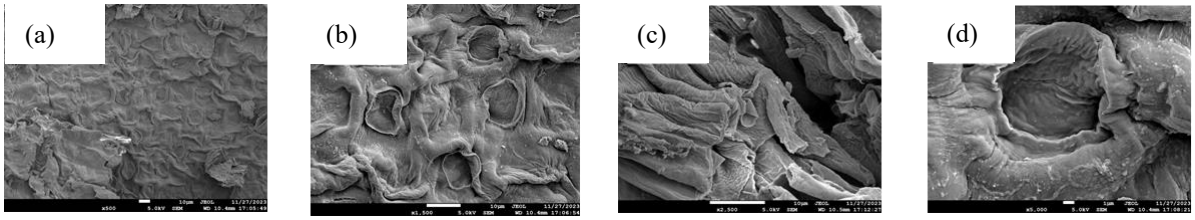


**Figure 21.** FE-SEM images of the surface morphology of *Padina* sp. after adsorption at pH 4, at different magnifications: (a)500x (b) 1500x (c) 2500x (d) 5000x.

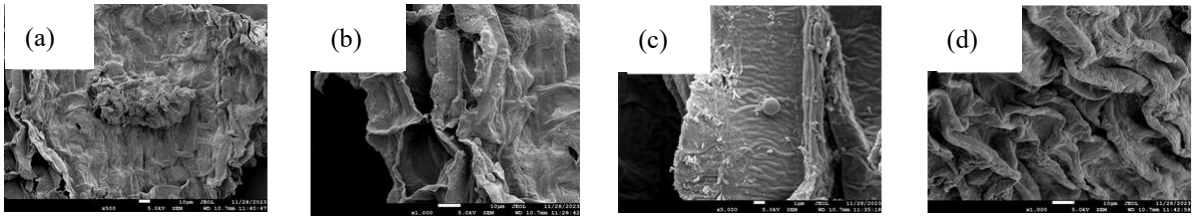


**Figure 22.** FE-SEM images of the surface morphology of *Padina* sp. after adsorption at pH 6, at different magnifications: (a)500x (b) 1000x (c) 1500x (d) 5000x.

There was adsorption of chromium ($Cr^{6+}$) and cadmium ($Cd^{2+}$) at the surface of the adsorbent, as indicated by the changes in pore size and surface texture. The pores at the adsorbent's surface were larger and their texture was smoother after biosorption.

**Adsorption Data**

*Effect of Drying Method on Heavy Metal Adsorption*

To study the capacity of seaweed (*Kappaphycus* sp.*, Padina* sp. and *Sargassum* sp.*)* as a biosorbent, the effect of the drying method on adsorption was investigated. This was done by drying all biosorbents using two different methods, oven drying and freeze drying.

The oven temperature was fixed at 60 °C for all samples, while the temperature used for freeze drying was fixed at -50 °C. As shown in **Figure 23**, the highest removal percentage for chromium was 19.8 %, with the freeze-dried *Padina* sp. samples. For cadmium, freeze-dried *Sargassum* sp. had the highest removal percentage of 75.2 %.

The increase in heavy metal adsorption was due to preservation of the functional groups in the adsorbent. Freeze drying appeared to be the most suitable approach for drying seaweed in order to preserve its nutritional content, minerals, and functional groups. In contrast, the use of high temperatures during the oven drying process resulted in the largest nutrient losses among all the samples that were treated, despite the fact that the ash and mineral contents were conserved [28]. This is because the high temperature used in oven drying inactivates polyphenol oxidase that is present in the samples [17].

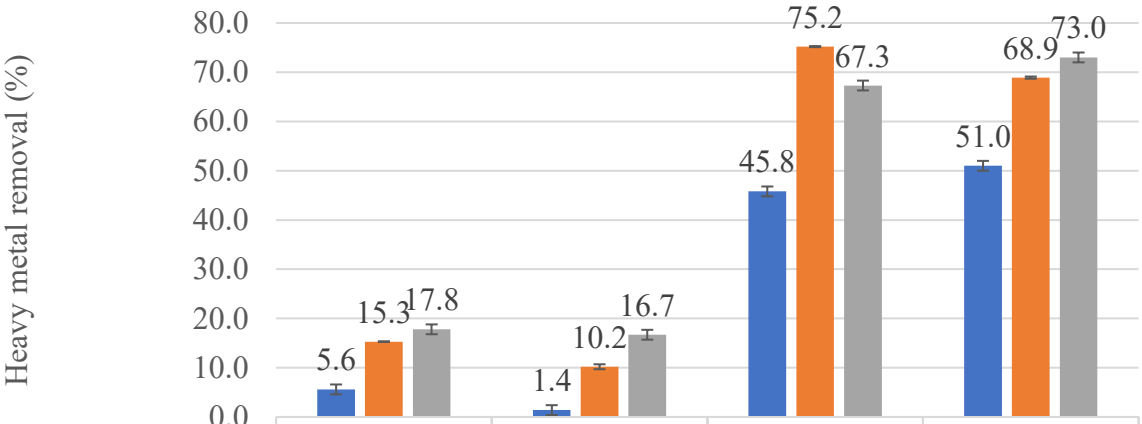


| | chromium ($Cr^{6+}$) | | cadmium ($Cd^{2+}$) | |
|---|---|---|---|---|
| | freeze | oven | freeze | oven |
| Kappaphycus sp. | 5.6 | 1.4 | 45.8 | 51.0 |
| Sargassum sp. | 15.3 | 10.2 | 75.2 | 68.9 |
| Padina sp. | 17.8 | 16.7 | 67.3 | 73.0 |

**Figure 23.** Effect of drying method (freeze drying and oven drying) on the adsorption capacity of seaweed species (*Kappaphycus* sp., *Sargassum* sp. and *Padina* sp.) towards chromium ($Cr^{6+}$) and cadmium ($Cd^{2+}$).

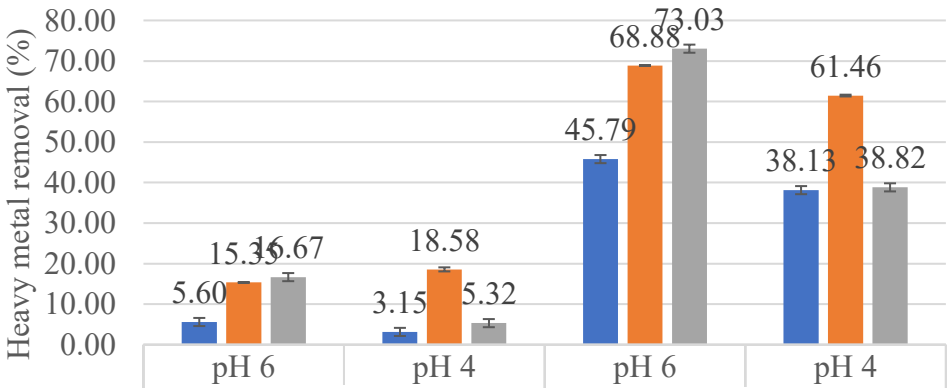


| | chromium ($Cr^{6+}$) | | cadmium ($Cd^{2+}$) | |
|---|---|---|---|---|
| | pH 6 | pH 4 | pH 6 | pH 4 |
| Kappaphycus sp. | 5.60 | 3.15 | 45.79 | 38.13 |
| Sargassum sp. | 15.35 | 18.58 | 68.88 | 61.46 |
| Padina sp. | 16.67 | 5.32 | 73.03 | 38.82 |

**Figure 24.** Effect of pH on the adsorption capacity of freeze-dried seaweed species (*Kappaphycus* sp., *Padina* sp., and *Sargassum* sp.) for chromium ($Cr^{6+}$) and cadmium ($Cd^{2+}$).

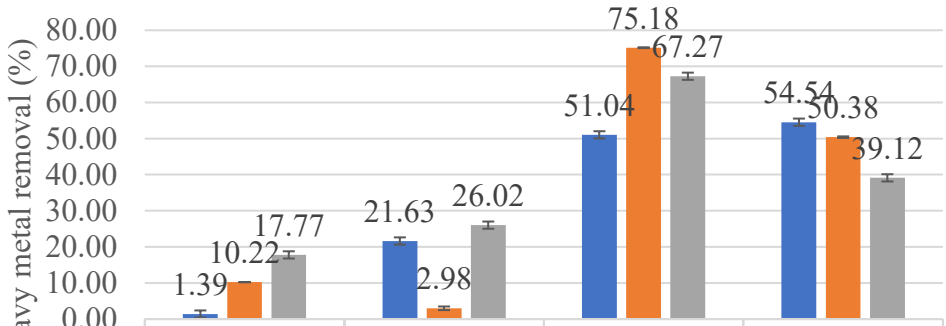


| | chromium ($Cr^{6+}$) | | cadmium ($Cd^{2+}$) | |
|---|---|---|---|---|
| | pH 6 | pH 4 | pH 6 | pH 4 |
| Kappaphycus sp. | 1.39 | 21.63 | 51.04 | 54.54 |
| Sargassum sp. | 10.22 | 2.98 | 75.18 | 50.38 |
| Padina sp. | 17.77 | 26.02 | 67.27 | 39.12 |

**Figure 25.** Effect of pH on the adsorption capacity of oven-dried seaweed species (*Kappaphycus* sp., *Padina* sp., and *Sargassum* sp.) for chromium ($Cr^{6+}$) and cadmium ($Cd^{2+}$).

*Effect of pH on Heavy Metal Adsorption*

To investigate the effect of pH on biosorption, a fixed amount of adsorbent (0.2 g) was used in 30 mL aqueous metal solution at pH 4 and 6. The negative percentage of removal may be attributed to the low initial concentration of chromium ions in the solution [52, 56]. This leads to desorption, where previously adsorbed ions are released into solution and displaced by other ions. In **Figure 24**, the highest percentage removal for chromium ($Cr^{6+}$) and cadmium ($Cd^{2+}$) was at pH 6, with removal percentages of 18.58 % and 73 % respectively. In **Figure 25** the highest percentage removal for chromium and cadmium solution was also at pH 6, with 17.8 % and 75.2 % respectively.

The negative removal percentage observed at certain conditions may be explained by desorption, which occurs when the initial concentration of metal ions in solution is too low to sustain adsorption equilibrium. In such cases, previously adsorbed ions may be released into the solution and displaced by competing ions, leading to an apparent negative removal efficiency [40-42].

Similar findings have been reported in heavy metal biosorption studies, where desorption was more pronounced at low ion concentrations due to weaker driving forces for mass transfer [53].

The influence of pH on biosorption was also evident in this study, with the highest removal of chromium ($Cr^{6+}$) and cadmium ($Cd^{2+}$) obtained at pH 6. This can be attributed to reduced competition between protons and metal cations for active binding sites on the adsorbent surface, as lower pH values result in protonation of functional groups such as –COOH and –OH, thereby reducing metal uptake [54-55]. At moderately acidic conditions (around pH 6), deprotonation of binding sites occurs, favouring the electrostatic attraction of metal cations and enhancing biosorption efficiency.

These results show that the adsorbent tended to take up more heavy metals at relatively neutral conditions. This implies that the surface of the adsorbent did not exhibit any strong positive or negative charges. In other words, a slightly positive or slightly negative adsorbent surface still allows adsorption [15-17]. At extremely low pH levels, the protonated cell wall ligand at the adsorbent's surface hindered the movement of metal ions due to repulsive forces. However, it was a different case at higher pH levels, where functional groups such as carboxyl, amino and sulfate which were exposed on the surface carried negative charges that attracted heavy metals to bind with them [26].

**Kinetic Study on Selected Samples**

The kinetic study was designed using a simplified approach, where only the most effective seaweed species (*Sargassum* sp.) prepared by freeze drying was selected. This design was chosen to reduce experimental complexity and to focus on the biosorbent with the highest removal efficiency, as confirmed by ICP-OES analysis. While it would have been possible to include all seaweed species for comparison, restricting the kinetic analysis to the best-performing biosorbent allowed for a more precise evaluation of the adsorption mechanism under optimised conditions. Based on the ICP-OES results, the optimum adsorption occurred at pH 6 in cadmium ($Cd^{2+}$) solution.

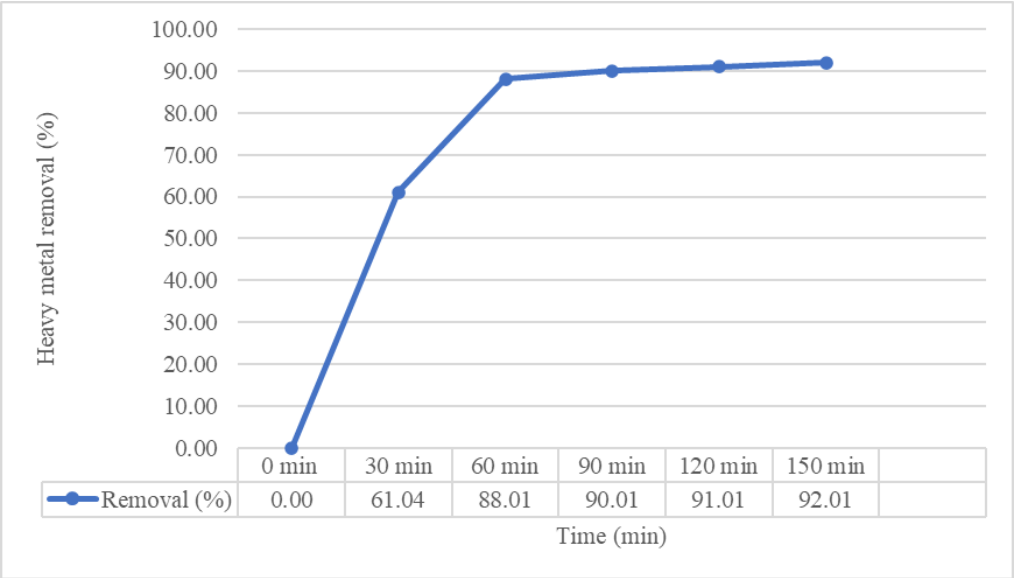


**Figure 26.** Percentage adsorption of cadmium ($Cd^{2+}$) by *Sargassum* sp. as a function of contact time, demonstrating a fit to the Langmuir isotherm model.

For the kinetic analysis, 5 mL of solution was sampled every 30 minutes for 3 hours, followed by dilution and ICP-OES determination [48]. The results revealed a sharp increase in removal efficiency at 30 minutes, after which the adsorption rate gradually declined until equilibrium was achieved. Similar findings were reported by Jayakumar et al. [9, 29], who observed that the adsorption of cadmium ($Cd^{2+}$) onto *Sargassum* sp. followed the Langmuir isotherm. This behaviour suggests that once most of the available active sites on the biosorbent surface were occupied by metal ions, further adsorption was increasingly limited. The plateau observed in the kinetic curve (**Figure 26**) therefore indicates saturation of the binding sites [13, 48–49].

However, some studies have shown that the effectiveness of the biosorbent is dependent upon the Langmuir parameters $q_m$, which indicates maximum adsorption capacity and $b$, the affinity constant. A biosorbent with a low $q_m$ and a high $b$ may be more effective than a biosorbent with a high adsorption capacity and a low binding affinity, particularly when dealing with metal ions at trace levels [22-24, 53-55].

## CONCLUSION

Surface morphology (FE-SEM) and functional group (FTIR) analyses collectively confirmed that freeze drying was the superior method for preparing the biosorbents, compared to oven drying. FE-SEM images demonstrated that the freeze-dried samples preserved cellular integrity, exhibited larger pore size distribution, and maintained a smoother surface, all of which are structural features associated with enhanced metal uptake. This observation is supported by previous studies by Huang *et al.,* (2025) [47] and Volesky, (2007) [56] which found that greater porosity and smoother surface morphology increased the accessibility of binding sites, thereby improving biosorption efficiency. Complementary FTIR spectra further verified the involvement of functional groups such as –OH, C=C, and –SO in heavy metal binding, as shifts in band positions indicated ionic interactions between the biomass and metal ions. Furthermore, the results highlighted the influence of pH on the biosorption process. Although a lower uptake was observed at pH 4 for both chromium ($Cr^{6+}$) and cadmium ($Cd^{2+}$), removal efficiency improved at pH 6. However, to determine whether the differences in adsorption between pH values were statistically significant, further statistical testing (e.g., ANOVA or t-test) is recommended to strengthen the interpretation. This will provide a more robust conclusion regarding the effect of pH on biosorption performance. Lastly, ICP-OES results identified *Sargassum* sp. as the most effective biosorbent among the tested species, with optimum adsorption observed with freeze-dried samples at pH 6. Given its abundance along coastal areas, *Sargassum* sp. represents a sustainable and practical candidate for large-scale heavy metal remediation.

## ACKNOWLEDGEMENT

The authors would like to thank Universiti Malaysia Sabah (UMS) for providing funding for this research project through Dana Cluster Grant Fasa 1/2023 No. DKP0035.

REFERENCES

1. Al-Dhabi, N. A. and Arasu, M. V. (2022) Biosorption of hazardous waste from the municipal wastewater by marine algal biomass. *Environmental Research*, **204**, 112115: 1–8.

2. Alemayehu, A. B., Thomas, K. E., Einrem, R. F. and Ghosh, A. (2021) The Story of 5d Metallocorroles: From Metal-Ligand Misfits to New Building Blocks for Cancer Phototherapeutics. *Accounts of Chemical Research*, **54(15)**, 3095–3107.

3. Mingu, N. Aziz, S. A., Stidi, E. Y., Majid, M. H. A., Idris, J. and Sarjadi, M. S. (2022) Study of Composition and Surface Morphology of Seaweed as Biosorbent: A Review. *J. Phys.: Conf. Ser.*, **4** (2314 012029), 1–7.

4. Al-Saeedi, S. I., Ashour, M. and Alprol, A. E. (2023) Adsorption of toxic dye using red seaweeds from synthetic aqueous solution and its application to industrial wastewater effluents. *Frontiers in Marine Science*, **10**, 1–20.

5. Bajpai, A., Atoliya, N. and Prakash, A. (2022) Genetically engineered microbes in micro-remediation of metals from contaminated sites. In *Elsevier eBooks*, 397–416.

6 Kuang, Y., Sheng, X., Bao, D., Gao, C., Guo, L., Pang, G., Chen, B. & Ma, Z. (2025) Gradient experiment reveals physiological stress from heavy metal zinc on the economically valuable seaweed Sargassum fusiforme. *Marine Environmental Research*, **204**, 106958: 1–10.

7. Bersch, K. L., DeMeester, K. E., Zagani, R., Chen, S., Wodzanowski, K. A., Liu, S., Mashayekh, S., Reinecker, H. C. and Grimes, C. L. (2021) Bacterial Peptidoglycan Fragments Differentially Regulate Innate Immune Signaling. *ACS Central Science*, **7(4)**, 688–696.

8. Brazesh, B., Mousavi, S. M., Zarei, M., Ghaedi, M., Ghaedi, M. and Hashemi, S. A. (2021) Biosorption. In *Elsevier eBooks*, 587–628.

9. Jayakumar, V., Govindaradjane, S., Rajamohan, N. and Rajasimman, M. (2021) Biosorption potential of brown algae, Sargassum polycystum, for the removal of toxic metals, cadmium and zinc. *Environmental Science and Pollution Research*, **29(28)**, 41909–41922.

10. Mingu, N., Evangeline Yvonne, S., Abd Majid, M. H. and Sarjadi, M. S. (2023) A review of antioxidant potential from seaweeds: Extraction, characterization, benefits and applications. *Food Research*, **6(4)**, 58–64.

11. Kumar, P. S. and Ngueagni, P. T. (2022) Removal of volatile organic carbon and heavy metols through microbial approach. In *Elsevier eBooks*, 285–308.

12. Sarangi, N. V., Rajkumar, R., Kumar, N. S., Arunkumar, P., Alromaeh, A. I., AlReshaidan, S. B. and Al-Fatesh, A. S. (2025) Seaweed biosorption: A green solution for heavy metal remediation in aquatic and soil environments. *Desalination and Water Treatment*, **321**, 101036, 1–10.

13. Liu, Y., Serrano, A. and Nancucheo, I. (2021) Biological treatment of mine-impacted waters on the context of metal recovery. In *Elsevier eBooks*, 499–522.

14. Mingu, N., Musa, N., Abd Majid, M. H., Idris, J. and Sarjadi, M. S. (2022) Composition and surface morphology study of seaweed as biosorbent. *IOP Conference Series: Earth and Environmental Science*, **1103**, 012007.

15. López-Hortas, L., Caleja, C., Pinela, J., Petrović, J., Sokóvić, M., Ferreira, I. C., Torres, M. D., DomíNguez, H., Pereira, E. and Barros, L. (2022) Comparative evaluation of physicochemical profile and bioactive properties of red edible seaweed Chondrus crispus subjected to different drying methods. *Food Chemistry*, **383** (132450), 1–12.

16. Mingu, N., Zakaria, N. A., Abd Majid, M. H. and Sarjadi, M. S. (2023) Characterization of Kappaphycus sp. and Padina sp. as biosorbents for heavy metal ions removal. *Science, Engineering and Health Studies*, **17(1)**, 1–7.

17. Mitra, S., Chakraborty, A., Tareq, A. M., Emran, T. B., Nainu, F., Khusro, A., Idris, A. M., Khandaker, M. U., Osman, H., Alhumaydhi, F. A. and Simal-Gandara, J. (2022) Impact of heavy metals on the environment and human health: Novel therapeutic insights to counter the toxicity. *Journal of King Saud University - Science*, **34(3)**, 101865: 1–21.

18. Ordóñez, J. I., Cortés, S., Maluenda, P. and Soto, I. (2023) Biosorption of Heavy Metals with Algae: Critical Review of Its Application in Real Effluents. *Sustainability*, **15(6)**, 5521. 1–14.

19. Ravichandran, K. S. and Krishnaswamy, K. (2021) Sustainable food processing of selected North American native berries to support agroforestry. *Critical Reviews in Food Science and Nutrition*, **63(20)**, 4235–4260.

20. Santos, S. S., Rodrigues, L. M., Costa, S. C. and Madrona, G. S. (2017) Antioxidant compounds

from blackberry (Rubus fruticosus) pomace: Microencapsulation by spray drying and pH stability evaluation. *Food Packaging and Shelf Life*, **11**, 69–76.

21. Bikker, P., Stokvis, L., Van-Krimpen, M., Van-Wikselaar, P. and Cone, J. (2020) Evaluation of seaweeds from marine waters in Northwestern Europe for application in animal nutrition. *Anim. Feed Sci. Technol.*, **263**, 114460.

22. Chan, P. T., Matanjun, P., Yasir, S. M. and Tan, T. S. (2018) Influence of drying techniques on antioxidant activity and phytochemical content in seaweed. *Food Chemistry*, **245**, 1376–1383.

23. Raza, A., Farrukh, S., Hussain, A., Khan, I., Othman, M. H. D. and Ahsan, M. (2021) Performance Analysis of Blended Membranes of Cellulose Acetate with Variable Degree of Acetylation for CO2/CH4 Separation. *Membranes*, **11(4)**, 245: 1–12.

24. Subermaniam, K., Lew, S. Y., Yow, Y., Lim, S., Yu, W. S., Lim, L. W. and Wong, K. (2023) Malaysian brown macroalga Padina australis mitigates lipopolysaccharide-stimulated neuroinflammation in BV2 microglial cells. *PubMed*, **26(6)**, 669–679.

25. Yang, Y., Zhang, M., Alalawy, A. I., Almutairi, F. M., Al-Duais, M. A., Wang, J. and Salama, E. (2021) Identification and characterization of marine seaweeds for biocompounds production. *Environmental Technology and Innovation*, **24**, 101848; 1–12.

26. Mingu, N., Saad, K. M., Mamat, H., Siddiquee, M. S., Abd Majid, M. H. and Sarjadi, M. S. (2024) Comparative Study of Drying Methods on Seaweeds (Kappaphycus sp. and Padina sp.) Based on Their Phytochemical and Polysaccharaide Content Located in Sabah: Comparative study of drying methods on Seaweeds. *Borneo Journal of Resource Science and Technology*, **14(1)**, 112–122.

27. Li, Y., Helmreich, B. and Horn, H. (2011) Biosorption of Cu(II) Ions from Aqueous Solution by Red Alga (Palmaria Palmata) and Beer Draff. *Materials Sciences and Applications*, **2**, 70–80.

28. Göksungur, Y., Üren, S. and Güvenç, U. (2005) Biosorption of cadmium and lead ions by ethanol treated waste baker's yeast biomass. *Bioresource Technology*, **96(1)**, 103–109.

29. Sathya, R., Arasu, M. V., Al-Dhabi, N. A., Vijayaraghavan, P., Ilavenil, S. and Rejiniemon, T. S. (2023) Towards sustainable wastewater treatment by biological methods - A challenges and advantages of recent technologies. *Urban Climate*, **47**, 101378: 1–18.

30. Deniz, F. and Karabulut, A. (2017) Biosorption of Heavy Metal Ions by Chemically Modified Biomass of Coastal Seaweed Community: Studies on Phycoremediation System Modeling and Design. *Ecological Engineering*, **106**, 101–108.

31. Montazer-Rahmati, M. M., Rabbani, P., Abdolali, A. and Keshtkar, A. R. (2011) Kinetics and equilibrium studies on biosorption of cadmium, lead, and nickel ions from aqueous solutions by intact and chemically modified brown algae. *Journal of Hazardous Materials*, **185(1)**, 401–407.

32. Azadi, M., Teimouri, A. and Mehranzadeh, G. (2016) Preparation, characterization and biocompatible properties of β-chitin/silk fibroin/ nanohydroxyapatite composite scaffolds prepared using a freeze-drying method. *RSC Adv.*, **6**, 7048–7060.

33. Badmus, U. O., Taggart, M. A. and Boyd, K. G. (2019) The effect of different drying methods on certain nutritionally important chemical constituents in edible brown seaweeds. *J. Appl. Phycol.*, **31**, 3883–3897.

34. Uribe, E., Vega-Gálvez, A., García, V., Pastén, A., Rodríguez, K., López, J. and Di Scala, K. (2020) Evaluation of physicochemical composition and bioactivity of a red seaweed (Pyropia orbicularis) as affected by different drying technologies. *Drying Technology*, **38(9)**, 1218–1230.

35. Indriyawati, N., Supriyanto and Nabwiyah, N. D. N. (2024) Nutritional composition of Sargassum sp. and Padina sp. *BIO Web of Conferences*, **127**, 03001.

36. Shao, Z. and Duan, D. (2022) The Cell Wall Polysaccharides Biosynthesis in Seaweeds: A Molecular Perspective. *Front. Plant Sci.*, **13**, 902823, 1–7.

37. Bixler, H. J. and Porse, H. (2011) A decade of change in the seaweed hydrocolloids industry. *Journal of Applied Phycology*, **23(3)**, 321–335.

38. Prashant, N., Sangwan, M., Singh, P. and Das, P. (2025) Anti-nutritional factors and heavy metals in edible seaweeds: Challenges, health implications, and strategies for safer consumption. *Journal of Food Composition and Analysis*, **140**, 107283, 1–13.

39. Khaled, A., El Naggar, M. E., El-Mekawy, A., El-Sikaily, A. and El Nemr, A. (2019) Morphological

and structural characterisation of Padina and Sargassum species using SEM and FTIR. *Algal Research*, **38**, 101393.

40. Rama Rao, K., Rengasamy, R. and Murthy, K. S. R. (2007) Cell wall polysaccharides of red, brown, and green seaweeds and their water-binding capacity. *Journal of Applied Phycology*, **19(5)**, 717–720.

41. Syaifudin, M., Moussa, M. G., Li, T. and Du, H. (2025) The impact of salinity on heavy metal accumulation in seaweed. Marine Pollution Bulletin, **214**, 117819, 1–18.

42. Roleda, M. Y., Marfaing, H., Desnica, N., Jorissen, H. and Nyberg, C. (2019) Variability in carrageenan content and morphology of carrageenophytes (Kappaphycus, Eucheuma). Journal of Applied Phycology, **31(2)**, 1313–1325.

43. Shao, Z. and Duan, D. (2022) The cell wall polysaccharides biosynthesis in seaweeds: A molecular perspective. *Frontiers in Plant Science*, **13**, 902823.

44. Silva, A. F. R., Abreu, H., Silva, A. M. S. and Cardoso, S. M. (2019) Effect of oven-drying on the recovery of valuable compounds from Ulva rigida, Gracilaria sp., and Fucus vesiculosus. *Marine Drugs*, **17(2)**, 90.

45. Chen, X., Chen, J., You, Q., Chen, F. and Xu, H. (2021) Advances in drying technology for food and agricultural products. *Critical Reviews in Food Science and Nutrition*, **61(13)**, 2113–2132.

46. Erbay, Z. and Icier, F. (2010) A review of thin layer drying of foods: Theory, modeling, and experimental results. *Critical Reviews in Food Science and Nutrition*, **50(5)**, 441–464.

47. Huang, L., Lee, J. -Y., Park, Y. -K. and Lee, J. (2025) Heavy metals in seaweed: Implications for health benefits, risks, and safety regulations. *Journal of Agriculture and Food Research*, **21**, 101830, 1–8.

48. Lewicki, P. P. (2006) Design of hot air drying for better foods. *Trends in Food Science & Technology*, **17(4)**, 153–163.

49. Mujumdar, A. S. (2015) Handbook of industrial drying (4th ed.). *CRC Press*.

50. Ratti, C. (2001) Hot air and freeze-drying of high-value foods: A review. *Journal of Food Engineering*, **49(4)**, 311–319.

51. Taboada, E., Fisher, P., Laurens, L. and Van Wagenen, J. (2010) Chemical composition of the edible seaweeds Ulva lactuca, Gracilaria changii, and Sargassum polycystum. *Food Chemistry*, **120(2)**, 491–498.

52. Ahalya, N., Ramachandra, T. V. and Kanamadi, R. D. (2003) Biosorption of heavy metals. Research Journal of Chemistry and Environment, **7(4)**, 71–79.

53. Anastopoulos, I. and Kyzas, G. Z. (2015) Progress in batch biosorption of heavy metals onto algae. *Journal of Molecular Liquids*, **209**, 77–86.

54. Feng, N. and Guo, X. (2012) Characterization of adsorptive capacity and mechanisms on adsorption of copper, lead and zinc by modified orange peel. *Transactions of Nonferrous Metals Society of China*, **22(5)**, 1224–1231.

55. Veglio, F. and Beolchini, F. (1997) Removal of metals by biosorption: A review. *Hydrometallurgy*, **44(3)**, 301–316.

56. Volesky, B. (2007) Biosorption and me. *Water Research*, **41(18)**, 4017–4029.